Eur. Phys. J. B (2025) 98:44
https://doi.org/10.1140/epjb/s10051-025-00889-3

THE EUROPEAN PHYSICAL JOURNAL B

Regular Article - Solid State and Materials

Structural, wettability, optical, and electrical modifications by varying precursor solutions of sprayed Co_3O_4 thin films for solar cell applications

Younes Nezzari[1], Warda Darenfad[1,a], Kamel Mirouh[1], Noubeil Guermat[2,3], and Nadir Bouarissa[4]

[1] Thin Films and Interfaces Laboratory (LCMI), University of Constantine 1, 25000 Constantine, Algeria
[2] Department of Electronics, Faculty of Technology, University of M'sila, University Pole, Road Bourdj Bou Arreiridj, 28000 M'sila, Algeria
[3] Laboratoire Des Etudes de Matériaux d'Electronique Pour Applications Médicales (LEMEAMED), Université de Constantine 1, 25000 Constantine, Algerie
[4] Laboratory of Materials Physics and Its Applications, University of M'sila, 28000 M'sila, Algeria

Received 10 January 2025 / Accepted 18 February 2025 / Published online 8 March 2025

1 Introduction

There are three crystalline forms of cobalt oxide (CoO, Co_3O_4, and Co_2O_3), Co_3O_4 is preferred for various applications, such as solar cells [1, 2], energy storage [3], gas sensors [4], and catalysts [5] due to its unique physicochemical properties. These include: (i) Co_3O_4 is a p-type semiconductor with a band gap ranging from 1.5 to 2.1 eV, making it well suited for optoelectronic applications like solar cells. This band gap allows efficient absorption of visible light, improving its functionality in photovoltaic devices. (ii) Compared to CoO and Co_2O_3, Co_3O_4 exhibits superior chemical stability under normal environmental conditions, making it more durable for devices such as solar cells and gas sensors, which need to maintain their performance over long periods. (iii) Co_3O_4 is known for its high catalytic activity, especially for oxidation and reduction reactions. This makes it very effective in catalytic applications and suitable for energy storage devices such as batteries and super-capacitors. (iv) Co_3O_4 has a spinel crystal structure, combining two oxidation states of cobalt (Co^{2+} and Co^{3+}). This structure offers interesting magnetic properties, which are important for magnetic device applications. (v) Co_3O_4 can be synthesized in various nano-structured forms, including nano-particles, nanowires, and thin films. This flexibility increases its surface area, which improves its performance in gas sensing, energy storage, and other technological applications. These combined properties make Co_3O_4 the preferred phase for advanced technological applications. Various deposition methods have been explored to produce Co_3O_4 thin films. In this study, we focus on spray pyrolysis, a method that offers advantages, such as low cost, no vacuum requirement, and ease of operation [6–8]. Spray parameters, including substrate temperature, deposition time, carrier gas flow rate, precursor molarity, and doping, significantly influence the physical properties of Co_3O_4 thin films. Many studies published in the literature have focused on the effects of deposition parameters on the structural, morphological, optical, and electrical properties of Co_3O_4 films produced using the chemical spray pyrolysis technique.

Among these parameters, the choice of cobalt precursor plays a very important and crucial role in determining the physical properties of Co_3O_4. Moreover, the choice of the cobalt precursor not only impacts the optical characteristics but also strongly affects the structural, surface, and electrical properties of the film. For example, Darenfad et al. [1] prepared Co_3O_4 thin films using aqueous cobalt nitrate with a molarity of 0.05 mol/L at a substrate temperature of 400 °C and an atomizer-to-substrate distance of 22 cm. They studied the optoelectronic and photovoltaic properties of the p-Co_3O_4/n-ZnO hetero-junction based on the deposition time of Co_3O_4 thin films. In another study, Daranfed et al. [2] demonstrated the effects of cobalt nitrate precursor concentrations ranging from 0.05 to 0.15 mol/L with the same substrate temperature (400 °C) and atomizer-to-substrate distance (22 cm) on the optoelectronic properties of Co_3O_4 thin films, using a cost-effective spray pyrolysis method for photovoltaic applications. Fan et al. [9] produced Co_3O_4 thin films by spray pyrolysis using 0.2 M cobalt acetate solution at a substrate temperature of 200 °C and

[a] e-mail: daranfed.warda@umc.edu.dz (corresponding author)

an atomizer–substrate distance of 7 cm for humidity sensor applications. Similarly, Kumar et al. [10] studied the effects of two different precursors, cobalt nitrate hexahydrate and cobalt chloride hexahydrate, both with a molarity of 0.1 mol/L, a substrate temperature of 400 °C and an atomizer-to-substrate distance of 12 cm, on the structural, optical, and electrical properties of Co_3O_4 thin films prepared by spray pyrolysis. To our knowledge and based on the literature, this is the first study to investigate the physical properties of Co_3O_4 thin films deposited using different cobalt sources (cobalt nitrate, cobalt chloride, and cobalt acetate) as absorber layers in thin-film solar cells. This highlights the novelty of our work and its contribution to advancing the understanding of how various cobalt precursors influence the characteristics of Co_3O_4 in solar cell applications. Surface wettability is an important aspect of thin-film surface properties and has significant implications for photovoltaic applications. Surfaces can be classified based on the contact angle (CA) of liquids: hydrophilic ($CA < 90°$) or hydrophobic ($CA > 90°$). Previous studies by Darenfad et al. [11] and Nezzari et al. [12] on p-type metal oxides such as CuO and Co_3O_4 confirmed that the hydrophobic nature of these oxides is beneficial for photovoltaic applications. They demonstrated that hydrophobicity improves the physical properties of absorbing thin films, making them more suitable for solar cell use. These intriguing results have motivated further investigations into the importance of hydrophobicity for absorber thin films in solar cells. To our knowledge, there is no study specifically exploring the effects of precursor solutions on the surface wettability of Co_3O_4 thin films prepared by spray pyrolysis for photovoltaic applications. In this study, we report the influence of various cobalt precursor sources, including cobalt nitrate, cobalt acetate, and cobalt chloride, on the physical properties of Co_3O_4 thin films. In addition, the fabrication process and detailed characterization results of p-Co_3O_4/n-ZnO hetero-junctions are presented.

2 Experimental procedure

Preparation of Co_3O_4 thin films by spray pyrolysis. This study explores the use of three different cobalt salts as precursor materials: cobalt nitrate hexahydrate ($Co(NO_3)_2.6H_2O$), cobalt chloride hexahydrate ($CoCl_2.6H_2O$), and cobalt acetate tetrahydrate ($(CH_3COO)_2Co.4H_2O$). All these precursors were obtained from Sigma-Aldrich with a high purity of 99.99%. Three separate solutions, each with a molarity of 0.05 M, were prepared by dissolving different cobalt salts in distilled water. The thin films were deposited on well-cleaned ordinary glass substrates, with the substrate temperature maintained at 400 °C. The distance between the atomizer and the substrate was set at 17 cm and the spray flow rate was controlled at 500 µl/min for a deposition time of 10 min. The spray pyrolysis chemical deposition technique is known for its simple experimental setup, as illustrated in Fig. 1.

After the deposition phase, the samples are subjected to a comprehensive analysis to study the characteristics of the deposited layers. This analysis uses several advanced techniques, including a Philips X'pert diffracto-meter operating with Cu Kα radiation ($\lambda = 1.5418$ Å) and a HORIBA LabRAM Raman spectrometer. These instruments are used to reveal the structural and compositional nature of the deposits on the substrate. Micro-Raman measurements are carried out at room temperature using the 633 nm excitation line of an argon ion laser, supplied by Renishaw. The thickness of our films was measured using a MicroXam-100 optical profilo-meter, ensuring accurate assessment of the deposited layers. For surface characterization, a Nanosurf Flex-Axiom C3000 atomic force microscope (AFM) in static (contact) mode was used at room temperature under ambient conditions. This technique allowed us to capture 3D images of representative samples, providing detailed visualization of the surface morphology. The 100 μm^2 (10 µm × 10 µm) scanning area facilitated high-resolution mapping, revealing fine details of surface features. In addition, the static contact angle was measured to assess the wettability of the thin films. A 5 µl droplet was placed on the sample at room temperature, illuminated by a LEYBOLD light source (6 V, 30 W), and the contact angle was recorded. In parallel, the optical properties of the films were studied using UV–visible spectroscopy in the wavelength range of 300–1000 nm, using a Shimadzu UV-3101 PC spectrophotometer to analyze light transmission. To evaluate the electrical properties, we used the Hall effect method to measure key parameters, such as resistivity, carrier concentration, and mobility at room temperature.

3 Results and discussion

3.1 Structural properties

Figure 2 presents X-ray diffraction (XRD) spectra of Co_3O_4 thin films deposited on glass substrates at a substrate temperature of 400 °C. These films were synthesized using three different cobalt precursors: cobalt chloride, cobalt nitrate, and cobalt acetate. All three thin films exhibit a polycrystalline nature, as evidenced by the presence of seven prominent diffraction peaks. These peaks correspond to the crystallographic planes (111), (220), (311), (400), (422), (511), and (440), with a dominant preferred orientation along the (311) plane. These diffraction peaks are in excellent agreement with the standard peaks of the cubic spinel structure Co_3O_4, as referenced by JCPDS card no. 42-1467, which is consistent with the results of several previous studies [1, 2, 13]. Moreover, the most stable Co_3O_4 phase was obtained, as no additional peaks corresponding to other cobalt oxides, such as CoO or Co_2O_3, were detected. This observation is consistent with the results reported

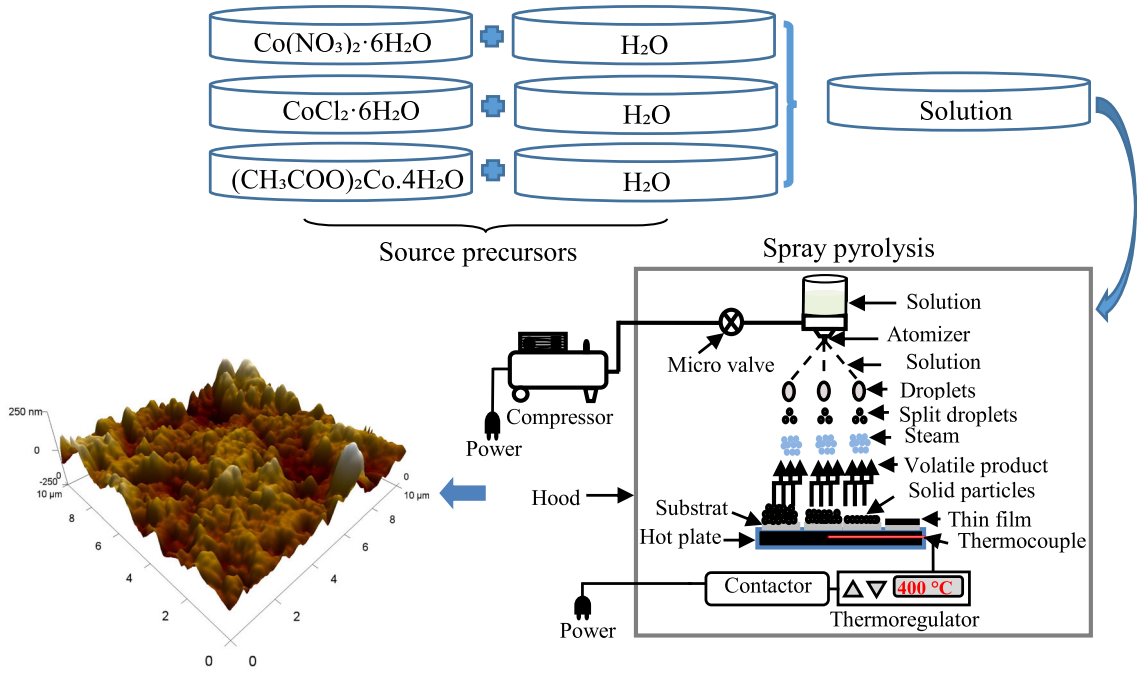

Fig. 1 Schematic diagram of the spray technique

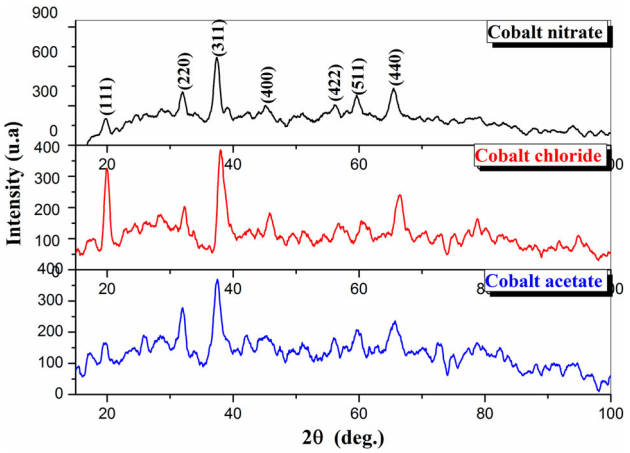

Fig. 2 XRD pattern of Co_3O_4 films deposited with different solutions

by Darenfad et al. [1, 2], who also used the spray pyrolysis technique. A notable variation in the intensity of the diffraction peaks was observed depending on the precursor used. In some cases, a decrease in peak intensity can be attributed to a reduction in the film thickness, which is influenced by the specific thermal decomposition kinetics of each precursor [14]. Indeed, cobalt chloride releases chloride ions (Cl^-) as decomposition by-products, which can disrupt the uniform formation of the crystal lattice by generating by-products that slow down crystallite growth. Cobalt acetate produces acetate groups (CH_3COO^-), which can also negatively influence the crystal quality by leaving organic residues or forming unstable intermediates. On the other hand, cobalt nitrate is distinguished by its ability to release gases, such as NO_x and O_2 during its thermal decomposition. These gases significantly improve the oxidation conditions of cobalt, thus promoting a more precise stoichiometry and limiting the formation of crystal defects. This optimization of growth conditions leads to the formation of well-ordered crystallites, highlighting structural imperfections. Therefore, the intensity of the diffraction peaks, especially for the (311) plane, is increased, reflecting improved crystal organization and more uniform film growth.

The crystallite size (D) of the films was determined using the following Debye–Scherrer equation [15]:

$$D = \frac{0.9\lambda}{\beta \cos\theta}, \tag{1}$$

where λ (0.15405 nm): the wavelength of the X-rays; θ: the Bragg diffraction angle; β is the width at half maximum (FWHM) in radians.

The strain (ε) and dislocation density (δ) of the synthesized films corresponding to the (311) crystallographic plane were determined using the following equations [1]:

$$\varepsilon = \frac{\beta \cos\theta}{4} \tag{2}$$

$$\delta = \frac{1}{D^2}. \tag{3}$$

Table 1 summarizes the calculated values for various structural parameters of the Co_3O_4 thin films prepared using the three different precursor sources. As shown

Table 1 Structural parameters of the Co_3O_4 films prepared using three different precursors

Precursor	2θ (°)	hkl planes	D (nm)	ε (10^{-3})	δ (nm^{-2})	d (nm)
Cobalt nitrate	37.39	(311)	9.688	3.577	0.0106	1113
Cobalt chloride	38.02	(311)	8.722	3.973	0.0131	782
Cobalt acetate	37.48	(311)	8.616	4.022	0.0135	724

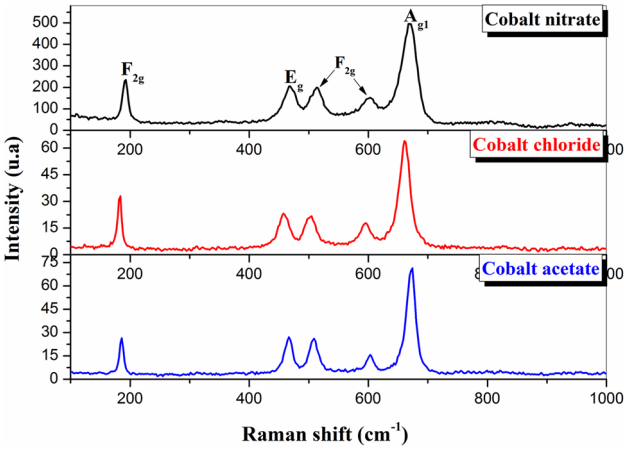

Fig. 3 Raman spectra of Co_3O_4 as a function of different precursors

in Table 1, the film synthesized with cobalt nitrate exhibits lower strain, calculated at 3.577×10^{-3}, and a high D of 9.688 nm compared to the films produced using the other cobalt sources. The reduction in strain is consistent with the preferred orientation observed in the film prepared with cobalt nitrate. It is well established that preferred orientation is often attributed to internal stress within the film [16]. Therefore, the use of cobalt nitrate in the deposition process likely promotes a more uniform and organized atomic arrangement within the film, reducing defects and dislocations (Table 1), which in turn results in larger crystallites and better overall material quality. This correlation between D and XRD data confirms the positive effect of cobalt nitrate on the structural properties of the film.

The Raman spectra of Co_3O_4 films prepared by different cobalt sources are presented in Fig. 3. As illustrated in this figure, the spectra clearly demonstrate the presence of five (05) distinct vibrational modes associated with the Co–O bond. The Raman peaks are located at approximately 190, 467, 512, 602, and 670 cm^{-1}, corresponding to the phonon modes with F_{2g}, E_g, and A_{1g} symmetries. These results are consistent with the data previously reported in the literature [17]. These modes arise from the vibrational motions of the Co^{2+} and Co^{3+} cations occupying tetrahedral and octahedral sites in the cubic lattice. This confirms the presence of a single-phase cubic spinel structure in Co_3O_4 [1, 2, 12]. Furthermore, the Raman spectra further corroborate the existence of the Co_3O_4 phase with cubic spinel structure, as previously deduced from the XRD analysis. Still in Fig. 3, comparing the Raman spectra of Co_3O_4 obtained from different precursors, a significant reduction in peak intensities is observed, especially for the A_{g1} peak. For the cobalt nitrate solution, the intensity of the A_{g1} peak is notably higher, measured at 441.72 a.u., compared to 61.08 a.u. and 52.67 a.u. for the cobalt chloride and cobalt acetate solutions, respectively. This decrease in the intensity of the A_{g1} Raman peak reflects variations in the crystal structure as well as the surface state of the material, which are directly influenced by the nature of the precursor used during the synthesis. The chemical composition of precursors, such as cobalt acetate and cobalt chloride, can have a significant impact on crystal formation and growth. These precursors can introduce defects or distortions within the crystal lattice (see Table 1), thereby disrupting the structural organization of Co_3O_4. These imperfections reduce the crystalline order and lead to a decrease in the intensity of vibrational modes, especially that associated with the A_{g1} mode.

3.2 Surface morphology and wettability analysis

Atomic force microscopy (AFM) was employed to examine the surface topography and roughness of our films. Figure 4 displays 3D AFM images of nanostructured Co_3O_4 over a 10 µm × 10 µm area, synthesized at 400 °C in ambient air using different cobalt precursors. The average surface roughness of the coatings increased progressively from 15.29 nm to 60.30 nm, and then to 65 nm, depending on whether cobalt nitrate, cobalt chloride, or cobalt acetate precursor solutions were used, respectively. This steady increase clearly demonstrates that the choice of precursor plays a critical role in determining the surface morphology of Co_3O_4 coatings. Surface roughness is a crucial factor for absorbent films, as it can enhance light trapping by increasing surface irregularities, leading to multiple reflections of incident light [12]. Light scattering caused by surface roughness extends the optical path length, improving light absorption in Co_3O_4 coatings [12]. Moreover, the distribution of peaks and valleys in the surface structure effectively traps more incident light into the internal structure of the coatings, thus increasing their intrinsic absorption properties and contributing to a better overall absorption performance [12]. Furthermore, based on AFM and X-ray diffraction analyses, especially in relation to D, it can be concluded that roughness is important for crystallization, but within optimal limits. From our study, we can infer that low surface roughness is favorable for the crystallization of Co_3O_4 produced by spray pyrolysis. Optimal crystallization appears to occur at lower roughness

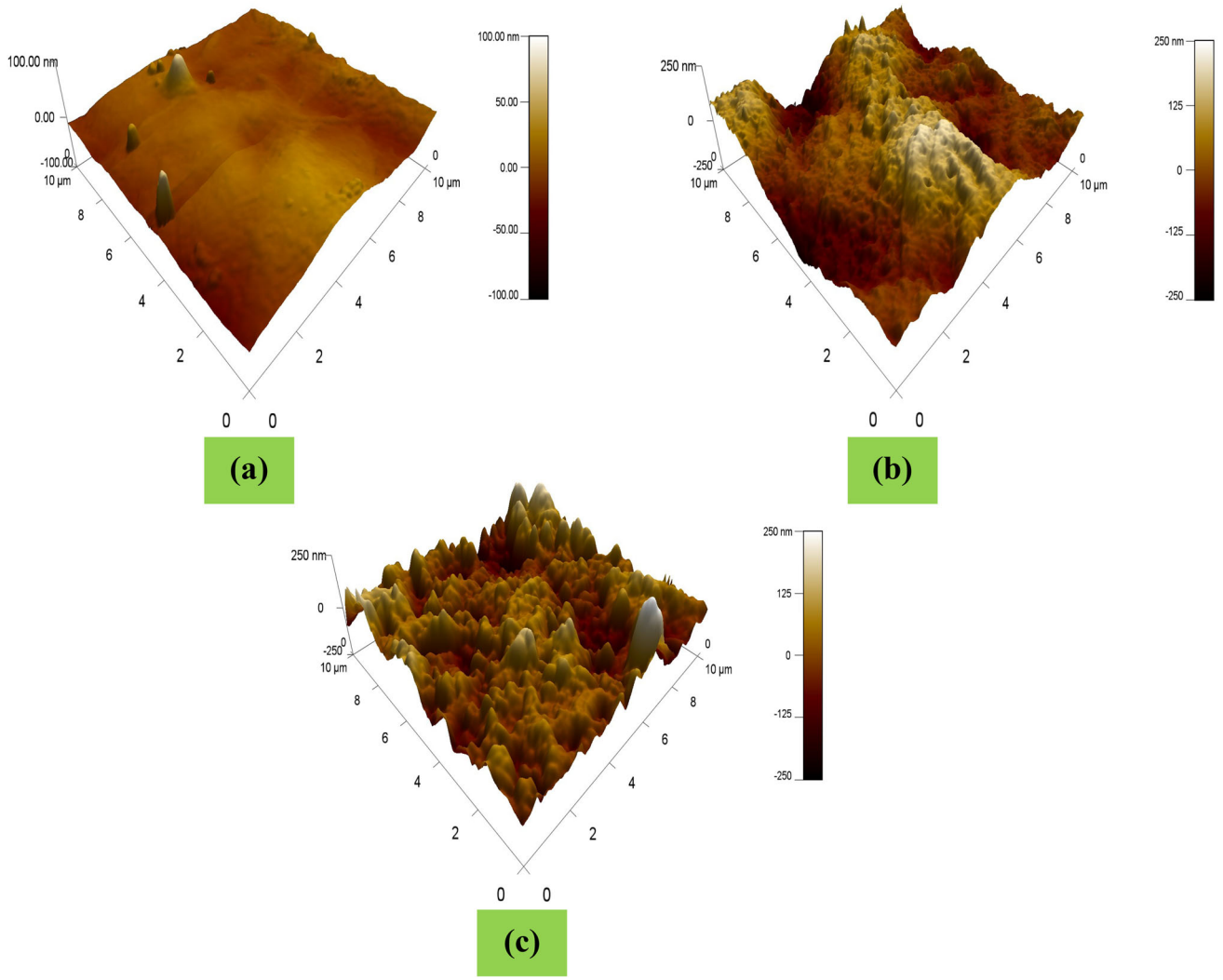

Fig. 4 AFM images of our thin films

levels, which favors a more uniform and well-organized crystal structure.

Figure 5 shows the static contact angle (CA) measurements of a water droplet, taken at four different points on the same surface for each prepared film. The results indicate an increase in contact angle values of 93°, 123°, and 134° for the samples derived from cobalt nitrate, cobalt chloride, and cobalt acetate, respectively. Additionally, all the films exhibit hydrophobic behavior (CA > 90°, [18, 19]). This hydrophobicity is attributed to the effect of surface roughness and crystallite size [12]. These findings are consistent with the AFM analysis presented in Fig. 4, which further supports the correlation between surface morphology and the hydrophobic properties of the films.

3.3 Optical analysis

An ultraviolet–visible (UV/Vis) spectrophotometer was employed to analyze the optical transmittance (T%) of the Co_3O_4 films synthesized using various precursors. Figure 6 illustrates the optical transmission spectra recorded across different films within the wavelength range of 300–900 nm. As observed, all the films exhibit low transmittance values, ranging between 0.96% and 6.09% in the visible wavelength region. Among them, the film prepared using cobalt nitrate demonstrates the lowest transparency, with a transmittance of just 0.96%, in comparison to the films prepared using cobalt chloride and cobalt acetate, which exhibit higher transmittance levels. The decrease in transmittance for the cobalt nitrate source is attributed to the presence of mixed oxidation states in the material, specifically Co_3O_4 ($(Co^{2+}, Co^{3+})_3O_4$), which imparts a black coloration and intensely absorbs incident photons as the film thickness (d) increases [1, 20]. Moreover, the low transmittance value obtained in this work for the cobalt nitrate precursor ($T = 0.96\%$) indicates that the film elaborated by spray efficiently captures light, a crucial property for enhancing the overall energy conversion efficiency in thin-film solar cells. We consistently

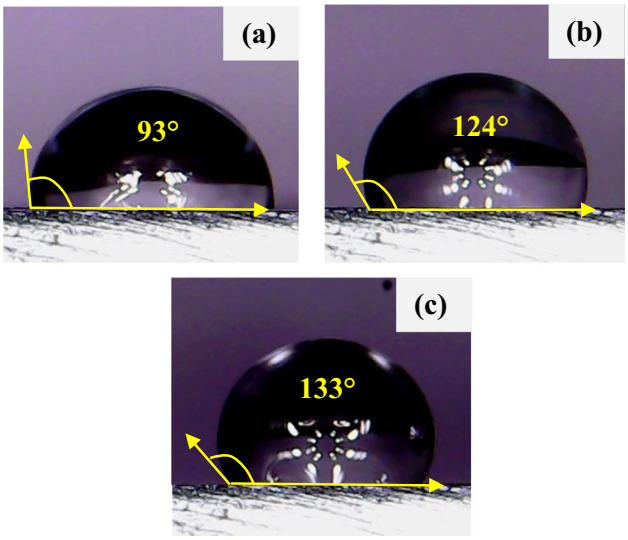

Fig. 5 Images of contact angles formed by water drops on Co_3O_4 thin films deposited with different precursors: (**a**) cobalt nitrate, (**b**) cobalt chloride and (**c**) cobalt acetate

observe the presence of a single absorption band in the transmission spectra between 700 and 900 nm, which is attributed to charge transfer ($O^{2-} \rightarrow Co^{3+}$) within the deposited films. This suggests the presence of a photonic band gap. In contrast, cobalt oxide typically exhibits two absorption bands in transmission spectra: one between 400 and 600 nm and another between 700 and 900 nm, corresponding to charge transfers ($O^{2-} \rightarrow Co^{2+}$) and ($O^{2-} \rightarrow Co^{3+}$), respectively [21]. However, in our films, only a single absorption band is observed. This discrepancy could be primarily attributed to the film thickness (Table 1), which plays a crucial role in determining optical absorption characteristics.

We calculated the optical band gap (Eg) for our films using the Tauc method [22], by plotting the contrast curve $(\alpha h\nu)^2$ as a function of photon energy ($h\nu$), as illustrated in Fig. 7.

Figure 8 highlights the impact of the type of cobalt precursor on the optical band gap (Eg) of Co_3O_4 films. The measured values range from 1.37 to 1.48 eV, which is consistent with results reported in the literature [1, 2]. Our study shows that the film obtained from cobalt nitrate exhibits the lowest band gap (1.37 eV), whereas those of the films prepared from cobalt chloride and cobalt acetate are slightly higher, reaching 1.48 eV and 1.46 eV, respectively. The reduction in Eg observed in the case of cobalt nitrate can be attributed to a decrease in structural deformation and an improvement in the crystalline arrangement. These characteristics also indicate better stoichiometry and more efficient oxidation, leading to a decrease in electrical resistivity. This aspect is crucial for photovoltaic applications, as a lower optical band gap allows for greater absorption of photons in the visible spectrum, thereby enhancing the material's performance as an absorbing layer in solar cells [23]. Conversely, the films deposited from cobalt chloride and cobalt acetate may contain structural defects (see Table 1), which affect the density of electronic states in the band gap and contribute to its increase.

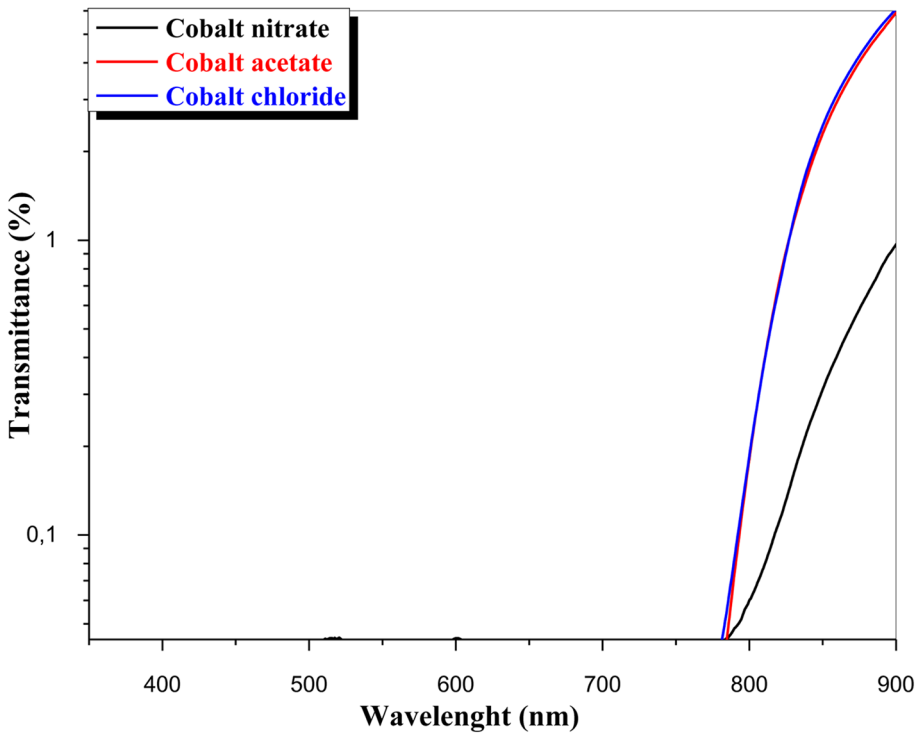

Fig. 6 Transmittance spectra of Co_3O_4 thin films prepared with different Co sources

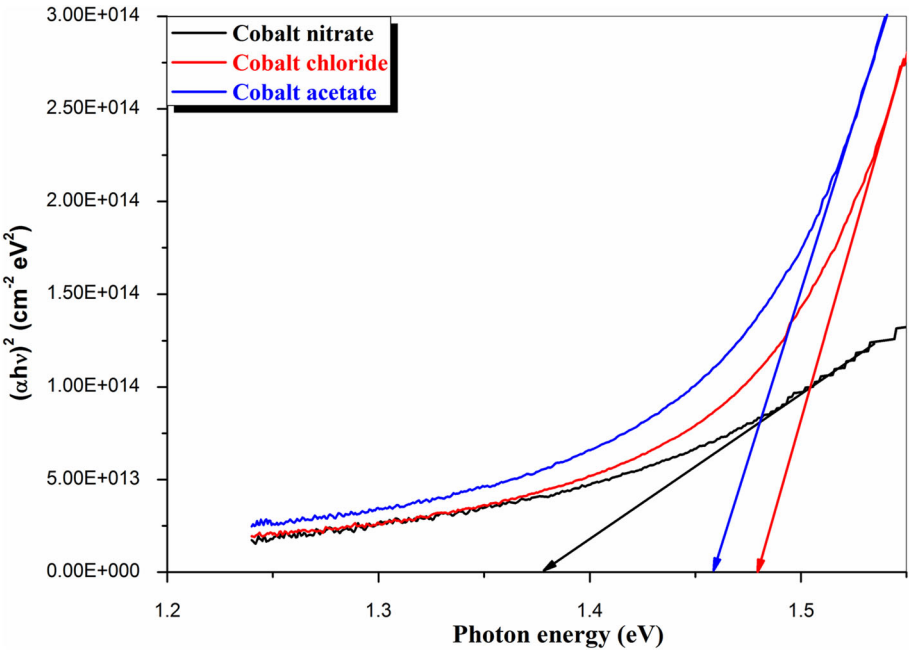

Fig. 7 Tauc's plots of Co_3O_4 thin films used for optical band-gap determination

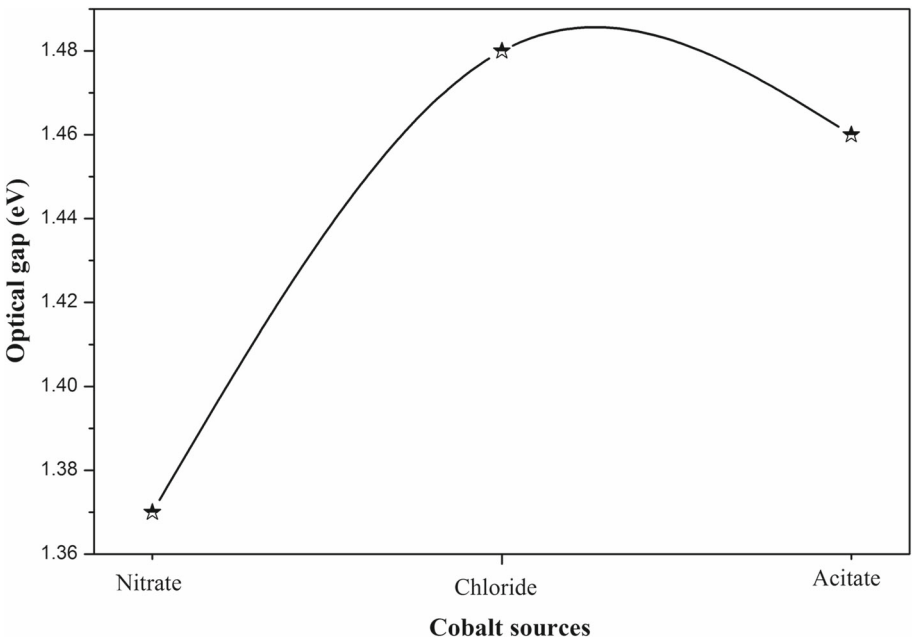

Fig. 8 Optical gap of Co_3O_4 films prepared with different sources

Furthermore, the widening of the Eg observed for the films obtained from zinc acetate and zinc chloride could be related to their surface roughness, compared to the film derived from cobalt nitrate, which has a less rough (Fig. 4). In conclusion, our results confirm that the choice of cobalt precursor plays a key role not only in the optical properties of Co_3O_4 films but also in their electrical and structural characteristics. To optimize their performance in optoelectronics and photovoltaic conversion, it is essential to consider these parameters in conjunction with other factors, such as deposition time [1] and precursor concentration [2].

The disorder in the film network is characterized by the width of the band known as the Urbach energy (E_U) [24, 25]. This can be estimated from the slope of the plot of $\ln(\alpha)$ as a function of $(h\nu)$, as illustrated in Fig. 9.

In Fig. 10, we have illustrated the variation of strain and disorder in the films depending on the different precursors used. It is evident that the disorder follows very consistently the strain trend, suggesting that the occurrence of strain in the films is strongly related to the presence of disorder. This phenomenon can be

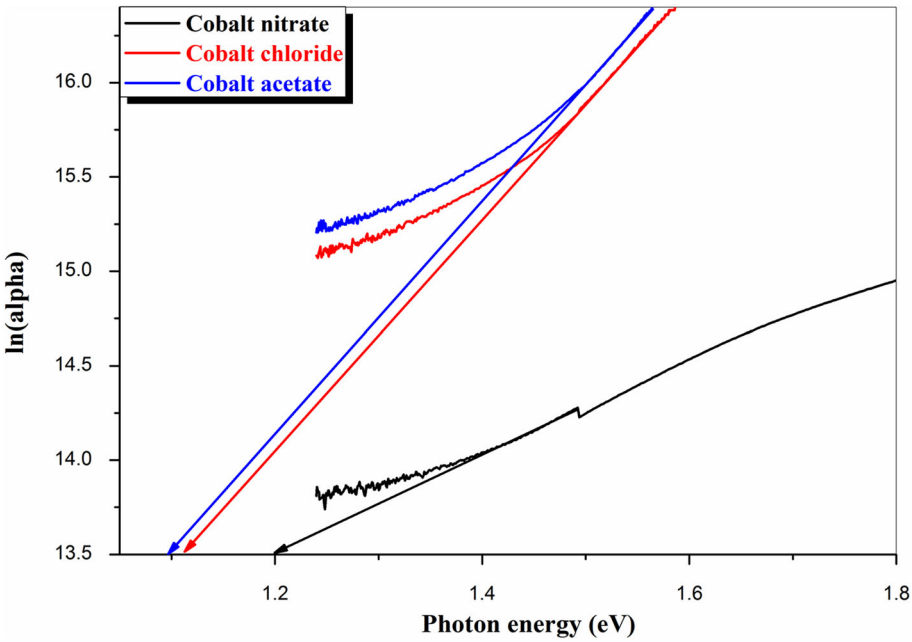

Fig. 9 Determination of disorder by extrapolation from the variation of ln(α) as a function of hυ

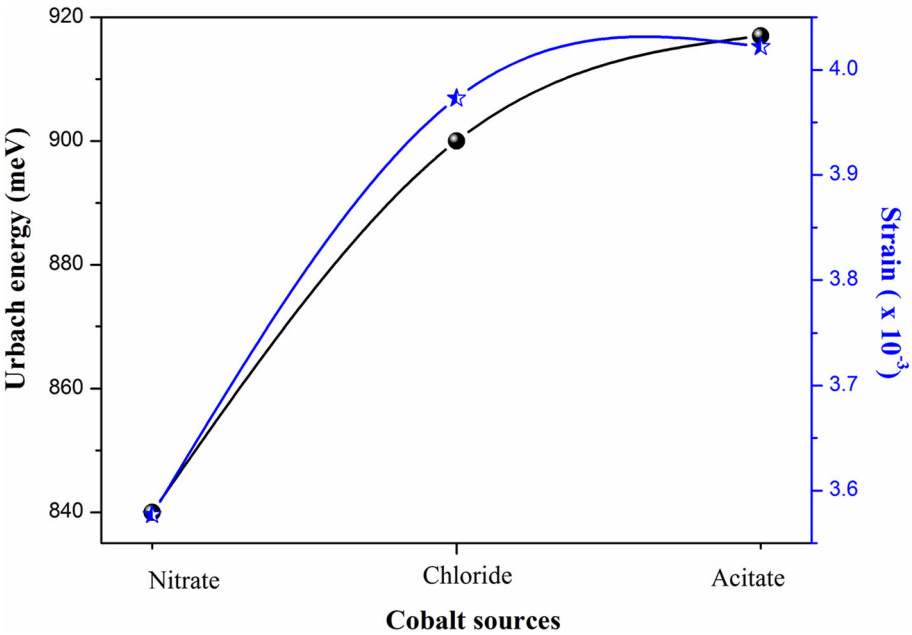

Fig. 10 Urbach energy or disorder and strain in Co_3O_4 films prepared with different sources

explained by the fact that disorder within the crystal structure, such as deviations in inter-atomic distances or bond angles from their ideal values, leads to the presence of weakly bonded or misaligned atoms. These structural defects disrupt the normal crystalline order, creating local distortions in the lattice parameters. These distortions manifest themselves as variations in the crystal lattice parameters, which induce internal forces in the material. These forces then cause strains in the films, potentially affecting their mechanical and structural properties.

3.4 Electrical analysis

The electrical properties of Co_3O_4 thin films were evaluated at room temperature using the Hall effect measurement technique. Table 2 presents the resistivity (ρ), mobility (μ), and free carrier concentration (n) values for Co_3O_4 films deposited from three different cobalt sources. The choice of cobalt source significantly influences electrical resistivity, which increases for cobalt chloride ($\rho = 3.001 \times 10^{1}$ Ω.cm) and cobalt acetate ($\rho = 3.716 \times 10^{1}$ Ω.cm) compared to cobalt nitrate ($\rho = 2.905 \times 10^{-1}$ Ω.cm). Transport properties are strongly affected by defect density, including strain, dislocations, and stacking faults, which are inherent to thin-film

Table 2 Electrical resistivity, free carriers concentration, and mobility of Co_3O_4 films deposited using different Co source

Precursor	ρ (Ω.cm)	μ (cm^2/vs)	n (cm^{-3})
Cobalt nitrate	2.905×10^{-1}	9.213	$2.333 \times 10^{+18}$
Cobalt chloride	$3.001 \times 10^{+1}$	3.538	$5.879 \times 10^{+15}$
Cobalt acetate	$3.716 \times 10^{+1}$	1.058	$1.587 \times 10^{+16}$

growth. The improved electrical conductivity is likely due to enhanced crystallinity in the Co_3O_4 films, as confirmed by the XRD results (Table 1). Larger crystallites reduce the number of grain boundaries, thereby lowering charge carrier transport barriers and improving conductivity. Additionally, electrical resistivity directly follows variations in carrier concentration, indicating that resistivity is primarily governed by free carrier concentration (Table 2). All the films exhibit p-type conductivity, as confirmed by the sign of the Hall coefficient [1]. The free carrier concentration in films derived from cobalt nitrate ($n = 2.333 \times 10^{18}$ cm^{-3}) is two and three orders of magnitude higher than that of films prepared from cobalt chloride ($n = 5.879 \times 10^{15}$ cm^{-3}) and cobalt acetate ($n = 1.587 \times 10^{16}$ cm^{-3}), respectively. This high carrier concentration, combined with improved crystallinity, significantly reduces the resistivity of the Co_3O_4 film obtained from cobalt nitrate. Furthermore, carrier mobility is influenced by crystallite size and surface roughness. A decrease in crystallite size and increased surface roughness, as observed in films derived from cobalt chloride and cobalt acetate, lead to a higher number of grain boundaries and irregularities, limiting charge carrier mobility and increasing resistivity. In contrast, films deposited from cobalt nitrate exhibit larger crystallites and a less rough surface, enhancing grain connectivity, reducing charge transport barriers, and thereby improving electrical conductivity. When compared to the literature, the minimum resistivity obtained in this study (2.905×10^{-1} Ω.cm) is lower than the values reported by Darenfad et al. [1] (7.94 Ω.cm), Nazzeri et al. [12] (28 Ω.cm), and Ravi Dhas et al. [20] (239.59 Ω.cm) for cobalt oxide thin films deposited via spray pyrolysis using cobalt nitrate as a precursor. Moreover, the resistivity achieved using the chemical spray pyrolysis method is also lower than that reported for films deposited by RF magnetron sputtering [26] and chemical bath deposition [27], where resistivity values range from 6.43 to 26.88 Ω.cm. These findings highlight the efficiency of spray pyrolysis in producing Co_3O_4 films with competitive resistivity suitable for photovoltaic applications.

4 Conclusions

Single-phase nanocrystalline Co_3O_4 thin films were successfully synthesized by spray pyrolysis using various cobalt precursors. X-ray diffraction analysis confirmed a cubic crystal structure with phase purity in all samples. Notably, the film produced from cobalt nitrate exhibited the largest crystallite size of 9.688 nm, surpassing those fabricated with other precursors. Raman spectroscopy further verified the formation of the Co_3O_4 spinel structure.

The Co_3O_4 films synthesized with cobalt nitrate also exhibited low surface roughness, while films produced using cobalt chloride and cobalt acetate exhibited significantly higher surface roughness. The static contact angles measured for all deposited films were consistently greater 90°, with the cobalt nitrate film exhibiting the highest contact angle, indicating better hydrophobicity. The Co_3O_4 thin film synthesized from cobalt nitrate exhibited very high absorbance, measured as only 0.96%, a low optical band gap of 1.32 eV, and an electrical resistivity of 2.905×10^{-1} Ω.cm. Therefore, cobalt nitrate was identified as the most efficient precursor to produce Co_3O_4 thin films suitable for solar cells, especially as an absorber layer.

Data availability There is no data. [Author's comment: The data that support the findings of this study are available upon reasonable request from the authors.].

References

1. W. Darenfad, N. Guermat, N. Bouarissa, F.Z. Satour, A. Zegadi, K. Mirouh, Improvement in optoelectronics and photovoltaic properties of p-Co_3O_4/n-ZnO heterojunction: effect of deposition time of sprayed Co_3O_4 thin films. J. Mater. Sci. Mater. Electron. **35**(162), 1–13 (2024). https://doi.org/10.1007/s10854-023-11909-2
2. W. Daranfed, N. Guermat, K. Mirouh, Experimental study in the effect of precursors in Co_3O_4 thin films used as solar absorbers. Ann Chim Sci Mat **44**, 121–126 (2020). https://doi.org/10.18280/acsm.440207
3. D. Yue, P. Rosaiah, K. Mallikarjuna, M. Rezaul Karim, J. Sh Alnawmasi, T. Jo Ko, G. Prakash Nunna, Inducing energy storage: Bimetallic MOF-derived Co_3O_4/NiO nanocomposites for advanced electrochemical applications. Polyhedron **260**, 117062 (2024). https://doi.org/10.1016/j.poly.2024.117062
4. Q. Xie, M. Liu, Q. Wang, P. Song, Fabrication of n-In_2O_3/p-Co_3O_4 composite nanofibers by electrospinning and their enhanced triethylamine sensing properties. Vacuum **227**, 113357 (2024). https://doi.org/10.1016/j.vacuum.2024.113357
5. P. Zhang, J. Liu, C. Zhou, Z. Xue, Y. Zheng, H. Tang, Z. Liu, Catalytic combustion of lean methane over different Co_3O_4 nanoparticle catalysts. Heliyon **9**, e21994 (2023). https://doi.org/10.1016/j.heliyon.2023.e21994
6. W. Darenfad, N. Guermat, K. Mirouh, Thoughtful investigation of ZnO doped Mg and co-doped Mg/Mn, Mg/Mn/F thin films: a first study. J. Mol. Struct.

1286, 135574 (2023). https://doi.org/10.1016/j.molstruc.2023.135574
7. I. Bellili, M. Mahtali, W. Darenfad, N. Guermat, The figure of merit improvement of (Sn, Co)–ZnO sprayed thin films for optoelectronic applications. Opt. Mater. **154**, 115785 (2024). https://doi.org/10.1016/j.optmat.2024.115785
8. W. Darenfad, N. Guermat, N. Bouarissa, K. Mirouh, Investigation of structural, morphological and optoelectronic properties of (Ni, Co)-doped and (Ni/Co) co-doped SnO_2 (110) sprayed thin films. J. Mol. Struct. **1317**, 138992 (2024). https://doi.org/10.1016/j.molstruc.2024.138992
9. X. Fan, J. Wang, S. Yang, C. Ma, Ce enhanced humidity-independent acetone-sensing properties of Co_3O_4 at a low operating temperature. Mater. Sci. Eng. B **298**, 116924 (2023). https://doi.org/10.1016/j.mseb.2023.116924
10. A. Kumar, P.P. Sahay, Precursor-dependent Spray-pyrolyzed Co_3O_4 thin films: comparative results on their structural, optical, and electrical properties. Braz. J. Phys. **52**, 101 (2022). https://doi.org/10.1007/s13538-022-01108-5
11. W. Darenfad, N. Guermat, K. Mirouh, Deposition time dependent physical properties of semiconductor CuO sprayed thin films as solar absorber. Eur. Phys. J. Appl. Phys. **99**, 17 (2024). https://doi.org/10.1051/epjap/20242302000
12. Y. Nezzari, W. Darenfad, K. Mirouh, N. Guermat, N. Bouarissa, R. Merah, Hydrophobic nickel doped Co_3O_4 sprayed thin films as solar absorber. Opt. Quant. Electron. **56**, 951 (2024). https://doi.org/10.1007/s11082-024-06930-6
13. S. Nasser Aziz, A.M. Abdulwahab, T. Shuga Aldeen, D.M. Ali Alqabili, Synthesis, characterization, and evaluation of antibacterial and antifungal activities of CuO-ZnO-Co_3O_4 nanocomposites. Heliyon **10**, e37802 (2024). https://doi.org/10.1016/j.heliyon.2024.e37802
14. A.A. Yadav, Electrochemical supercapacitive performance of spray deposited Co_3O_4 thin film nanostructures. Electrochim. Acta **232**, 370–376 (2017). https://doi.org/10.1016/j.electacta.2017.02.157
15. N. Guermat, W. Darenfad, K. Mirouh, M. Kalfallah, M. Ghoumazi, Super-hydrophobic F-doped SnO_2 (FTO) nanoflowers deposited by spray pyrolysis process for solar cell applications. J. Nano Electron. Phys. **15**, 05013 (2022). https://doi.org/10.21272/jnep.14(5).05013
16. I.B. Kherchachi, A. Attaf, H. Saidi, A. Bouhdjer, H. Bendjedidi, Y. Benkhetta, R. Azizi, Structural, optical and electrical properties of Sn_xS_y thin films grown by spray ultrasonic. J. Semicond. **37**, 032001 (2016). https://doi.org/10.1088/1674-4926/37/3/032001
17. J. Chen, H. Du, J. Zhang, X. Lei, Y. Wang, S. Su, Z. Zhang, P. Zhao, Influence of deposition temperature on crystalline structure and morphologies of Co_3O_4 films prepared by a direct liquid injection chemical vapor deposition. Surf. Coat. Technol. **319**, 110–116 (2017). https://doi.org/10.1016/j.surfcoat.2017.04.004
18. Z. Belamri, W. Darenfad, N. Guermat, Molarity dependence of solution on structural and hydrophobic properties of ZnO nanostructures. Eur. Phys. J. Appl. Phys. **99**, 10 (2024). https://doi.org/10.1051/epjap/2024230146
19. Z. Belamri, W. Darenfad, N. Guermat, Impact of annealing temperature on surface reactivity of ZnO nano-structured thin films deposited on aluminum substrate. J Nano-Electron Phys **15**, 02026 (2023). https://doi.org/10.21272/jnep.15(2).02026
20. C. Ravi Dhas, R. Venkatesh, R. Sivakumar, A. Moses Ezhil, C. Sanjeeviraja, Effect of solution molarity on optical dispersion energy parameters and electrochromic performance of Co_3O_4 films. Opt. Mater. **72**, 717–429 (2017). https://doi.org/10.1016/j.optmat.2017.07.026
21. S.A. Makhlouf, Z.H. Bakr, K.I. Aly, M.S. Moustafa, Structural, electrical and optical properties of Co_3O_4 nano-particles. Superlattice. Microst. **64**, 107–117 (2013). https://doi.org/10.1016/j.spmi.2013.09.023
22. N. Guermat, W. Darenfad, K. Mirouh, N. Bouarissa, M. Khalfallah, A. Herbadji, Effects of zinc doping on structural, morphological, optical and electrical properties of SnO_2 thin films. Eur. Phys. J. Appl. Phys. **97**, 14 (2022). https://doi.org/10.1051/epjap/2022210218
23. S.K. Jasmin Vijitha, K. Mohanraj, R.P. Jebin, Structural, optical, and surface modifications by varying precursor concentrations on spray deposition of In doped Co_3O_4 thin films for electro chemical application. Chem. Phys. Impact **6**, 100143 (2023). https://doi.org/10.1016/j.chphi.2022.100143
24. N. Guermat, W. Daranfed, I. Bouchama, N. Bouarissa, Investigation of structural, morphological, optical and electrical properties of Co/Ni co-doped ZnO thin films. J. Mol. Struct. **1225**, 129134 (2021). https://doi.org/10.1016/j.molstruc.2020.129134
25. W. Darenfad, N. Guermat, K. Mirouh, Effect of Co-doping on structural, morphological, optical and electrical properties of p-type CuO films. J. Nano Electron. Phys. **15**, 06009 (2023). https://doi.org/10.21272/jnep.15(6).06009
26. J. Olejníček, J. Šmíd, R. Perekrestov, P. Kšírová, J. Rathouský, M. Kohout, M. Dvořáková, Š Kment, K. Jurek, M. Čada, Z. Hubičk, Co_3O_4 thin films prepared by hollow cathode discharge. Surf. Coat. Technol. **366**, 303–310 (2019). https://doi.org/10.1016/j.surfcoat.2019.03.010
27. E. Turan, E. Zeybekoğlu, M. Kul, Effects of bath temperature and deposition time on Co_3O_4 thin films produced by chemical bath deposition. Thin Solid Films **692**, 137632 (2019). https://doi.org/10.1016/j.tsf.2019.137632